Time Domain Analysis of Elastic Nonlinearity in Concrete Using Continuous Waves

(Article begins on next page)

09 May 2024

We are IntechOpen,
the world's leading publisher of
Open Access books
Built by scientists, for scientists

4,200
Open access books available

116,000
International authors and editors

125M
Downloads

154
Countries delivered to

Our authors are among the

TOP 1%
most cited scientists

12.2%
Contributors from top 500 universities

CLARIVATE ANALYTICS

BOOK CITATION INDEX

INDEXED

WEB OF SCIENCE™

Selection of our books indexed in the Book Citation Index
in Web of Science™ Core Collection (BKCI)

Interested in publishing with us?
Contact book.department@intechopen.com

Numbers displayed above are based on latest data collected.
For more information visit www.intechopen.com

Chapter

Time Domain Analysis of Elastic Nonlinearity in Concrete Using Continuous Waves

Mourad Bentahar, Charfeddine Mechri, Paola Antonaci,
Antonio Gliozzi and Marco Scalerandi

Abstract

Concrete and consolidated granular media in general exhibit a strong nonlinear hysteretic elastic behavior when excited by ultrasonic wave perturbations. Due to the sensitivity of their elastic properties to the small changes that can appear in their microstructure, the dynamic stress-strain relationship considered at low strains is affected by the presence of microcracks and hence the progression of damage. Tracking the nonlinear behavior can be made through the dependence on the excitation amplitude of the amplitude of higher order harmonics or of the resonance frequency of the sample. The present chapter shows a time domain analysis of elastic nonlinearity based on the break of the superposition principle when ultrasonic continuous waves are propagating in concrete samples. The latter, which can be of different microstructures (grain sizes, mortar, or polymer matrix), helps to understand the physical mechanisms involved in the different nonlinear elastic responses.

Keywords: concrete, damage progression, nonlinear ultrasound, nonlinear elasticity, microcracking, nondestructive testing

1. Introduction

Numerous experimental observations have shown that microinhomogeneous media manifest a "new" nonlinear elastic behavior different from the one explained by the classical theory of nonlinear elasticity proposed by Landau and applicable to homogeneous and crystalline media. The "new" properties, described in the framework of the nonlinear mesoscopic elasticity (NME) formalism, include most types of rocks, concrete, bones, damaged metals, and composites, which manifest the same macroscopic observations despite the existing differences in their microstructures and chemical constituents [1–8]. Indeed, all these materials share the characteristic of being complex with contacts, or microdefects (i.e., cracks), grain boundaries, dislocations, etc.

Observations on these materials concern quasi-static and dynamic acoustic experiments. In quasi-static tests, the stress-strain relationship is governed by an unusual multivalued function where the observed hysteretic loop contains small inner loops showing the presence of a memory effect [9]. In dynamic experiments with a propagating acoustic wave, the proportionality between input and output

elastic waves is no longer valid. In such case, wave propagation (or even in standing wave conditions) is accompanied by the generation of amplitude dependent higher harmonics and sidebands [6, 10]. In addition, in resonance experiments, the increase in the dynamic perturbation creates a decrease in the elastic modulus of the propagating medium. This effect, which might be local or global, is observed through a decrease in the resonance frequency showing thus a softening in the elastic properties with an increase in damping around the excited resonance mode [11]. For relatively large excitation amplitudes, in the reversible regime, experiments show the presence of conditioning which means that the softening of elastic properties persists even when the excitation is switched off. In this case, at a given excitation amplitude, it takes seconds to minutes to stop the softening process and leads the medium into a new "equilibrium" state. The conditioning stops when the excitation is switched off. In this case, the medium needs minutes to days (depending on its state) to go back to its initial elastic state. This process is called relaxation and evolves in log-time [11–13].

So far in the literature, the aforementioned nonlinear effects have all been grouped into the same class in contrast with the classical nonlinearity well described by the Landau theory. However, a link has been postulated between the macroscopic nonlinear response and the microstructure of the different media [14]. Neutron scattering measurements have confirmed that the nonlinear behavior is localized in small regions close to discontinuities [15]. The observed regions might have different properties which makes the physical mechanisms described by the constitutive equation different. This makes the development of research around the existing relationship between the microscopic features and the different macroscopic observations interesting for basic research and for microcracks diagnosis in complex media.

Based on the above definitions, concrete as a consolidated granular medium is complex. Indeed, it exhibits a complicated nonlinear elastic behavior including hysteresis, harmonics generation, loss of reciprocity, etc. The complex structure of concrete can be seriously affected when damage is present. The latter, which can be of different origins, leads to important changes in the quasi-static (for advanced damage stages) and dynamic (for early damage stages) responses of concrete. Steel corrosion in reinforced concrete elements, mechanical stresses, thermal stresses, chemical attack by expansive agents, etc. have all negative effects on the concrete load carrying capacity, since they all lead to an increase in crack density and propagation. In this chapter, we propose to study the efficiency of a time domain analysis of elastic nonlinearity using continuous waves propagating in progressively damaged concrete samples.

2. Classical nonlinear theory

2.1 Stress-strain relations

In the approximation of small deformations, the free energy of an elastic system can be expanded as a power series with respect to the strain tensor. The general expression for the free energy of an isotropic body in the third approximation can be reduced by the convention of Einstein notation to

$$F = f_0 + C_{ijkl}\ \epsilon_{ij}\epsilon_{kl} + C_{ijklmn}\ \epsilon_{ij}\epsilon_{kl}\epsilon_{mn} \tag{1}$$

where f_0 is the constant, and C_{ijkl} and C_{ijklmn} are, respectively, the second and third order elastic tensors. For small strain amplitudes, the cubic term in the elastic energy can be neglected and the free energy reduces to

$$F = f_0 + C_{ijkl}\, \epsilon_{ij}\epsilon_{kl} \tag{2}$$

In the specific case of isotropic materials, the expression could be further reduced as

$$F = f_0 + \mu\, \epsilon_{ij}{}^2 + \frac{1}{2}\, \lambda\, \epsilon_{ii}{}^2 \tag{3}$$

where μ and λ are the Lamé coefficients.

At larger but still infinitesimal strains, the contribution of the third-order elastic term in the free energy expansion can no more be neglected. In such a case, the general expression for an isotropic medium becomes

$$F = f_0 + \mu\, \epsilon_{ij}{}^2 + \frac{1}{2}\, \lambda\, \epsilon_{ii}{}^2 + \frac{1}{3}\, A\, \epsilon_{ij}\, \epsilon_{ik}\epsilon_{kl} + B\, \epsilon_{ij}{}^2\epsilon_{ii} + \frac{1}{3}\, C\, \epsilon_{ii}{}^3 \tag{4}$$

where A, B, and C are the components of the third order elastic tensor for isotropic bodies. Consequently, the components of the stress tensor, obtained deriving the free energy with respect to strain are

$$\sigma_{ij} = \frac{\partial F}{\partial \epsilon_{ij}} = 2\mu\, \epsilon_{ij} + \frac{1}{2}\, \lambda\, \epsilon_{ii}\, \delta_{ij} + \frac{1}{3}\, A\, \epsilon_{ik}\epsilon_{kl} + 2\, B\, \epsilon_{ij}\, \delta_{ij} + C\, \epsilon_{ii}{}^2\delta_{ij} \tag{5}$$

Since strains are still infinitesimal, the corresponding elastic constants of the medium are

$$K_{ijkl} = \frac{\partial \sigma_{ij}}{\partial \epsilon_{kl}} \tag{6}$$

In the 1-D case, these equations reduce to the compressional stress σ

$$\sigma = (2\mu + \lambda)\, \epsilon + \left(\frac{1}{3}A + 3B + C\right)\epsilon^2 \tag{7}$$

The elastic modulus becomes

$$K = K_0(1 + \beta\epsilon) \tag{8}$$

K_0 is the Young modulus, and $\beta = \frac{\frac{1}{3}A + 3B + C}{2\mu + \lambda}$ is the quadratic nonlinear coefficient for longitudinal waves in isotropic media. Note that higher order terms of the elastic modulus can be obtained if we develop the free energy to the fourth order. In such a case, the modulus K would be $K = K_0(1 + \beta\epsilon + \delta\epsilon^2 + \dots)$, where $\delta = \frac{3l + 2m}{2\mu + 2\lambda}$ is the cubic nonlinear coefficient and l, m are the 3rd order elastic constants (called Murnaghan constants).

2.2 Wave equation

In the 1-D case, the equation of motion corresponding to a longitudinal plane wave propagating in a quadratic nonlinear medium can be written as

$$\frac{\partial^2 u}{\partial x^2} - \frac{1}{C_L^2}\frac{\partial^2 u}{\partial t^2} = -2\beta\frac{\partial^2 u}{\partial x^2}\frac{\partial u}{\partial x} \tag{9}$$

where C_L is the wave speed in the linear medium. Eq. (9) can be rewritten as

$$\frac{\partial^2 u}{\partial t^2} = C_L^2 \frac{\partial^2 u}{\partial x^2}\left[1 + 2\beta\,\frac{\partial u}{\partial x}\right] = C^2 \frac{\partial^2 u}{\partial x^2} \tag{10}$$

where $C^2 = C_L^2\left[1 + 2\beta\,\frac{\partial u}{\partial x}\right]$ is the wave speed. Note that, when higher nonlinear parameters are considered, the wave speed becomes $C^2 = C_L^2\left[1 + 2\beta\,\frac{\partial u}{\partial x} + 3\delta\left(\frac{\partial u}{\partial x}\right)^2\right]$. The velocity then becomes strain dependent and could be affected by any change in the strain amplitude of the propagating wave as a consequence of the change in the elastic modulus.

$$\frac{C^2 - C_L^2}{C_L^2} = \beta\epsilon + \delta\epsilon^2 \tag{11}$$

As a consequence, in the case of a nondispersive medium, the same dependence could be observed and measured for the resonance frequency, w_r, the latter being proportional to the velocity

$$\frac{C^2 - C_L^2}{C_L^2} \propto \frac{w_r^2 - w_L^2}{w_l^2} \propto 2\frac{w_r - w_L}{w_L} \tag{12}$$

The strain dependence of velocity is resulting in a shift of the resonance frequency when strain (or stress) amplitude increases. Therefore, the relation between the resonance frequency shift and the strain amplitude could be written as

$$<\frac{w_r - w_L}{w_L}> \propto \beta <\epsilon(t)> + \delta <\epsilon^2(t)> \tag{13}$$

When the excitation is considered as a sinusoidal function, the frequency shift could be reasonably dependent on the higher order expansion term, where $\delta <\epsilon^2(t)> = \frac{1}{2}\,\delta\,\epsilon_{max}^2$, which makes $\frac{w_r - w_L}{w_L} \propto \frac{1}{2}\,\delta\,\epsilon_{max}^2$.

3. Nonclassical nonlinear wave propagation in solids

The above discussed theory revealed to be nonsufficient to describe nonlinear behavior of elastic waves in diverse solids (concrete, cracked metals or composites, rocks, etc.). Indeed, these materials revealed that they belong to the class of nonlinear mesoscopic elastic materials (NMEM), where several experimental observations are in contradiction with the classical Landau theory expectations. In quasi-static stress-strain experiments (performed on sandstone, for instance), the dependence of stress on strain was nonlinear, hysteretic and showed the presence of memory effect [16]. Such evolution cannot be predicted in the framework of classical nonlinear Landau theory. Therefore, we need to introduce an additional term into the definition of stress by taking into account new parameters such as the stress dependence on the sign of the strain rate.

In addition to the quasi-static behavior described above, other observations suggest that nonlinearity in NMEM materials should have a different origin from that of atomistic nonlinearity and should therefore be related to the material structure. Most of these experiments are showing an anomalous dynamic behavior in NMEM materials, that is, when a time dependent perturbation is applied. In the different work in the literature, there is an agreement about the fact that most undamaged materials such as intact aluminum, Plexiglas, and monocrystalline solids show only a very small

nonlinear response related to strain at the atomic scale. In this range, their behavior is well described by the Landau theory. Evidence of such nonlinearity is only manifested at moderately high strain levels. Indeed, when these materials are microdamaged, their behavior at strain amplitudes $\varepsilon > 10^{-7}$ is more similar to that of Berea sandstone. Here, we should note that classical nonlinearity remains present, and as strain grows larger, its effect is hidden by stronger effects due to the presence of hysteresis. The following equation was therefore written as:

$$\frac{\partial^2 u}{\partial t^2} = C_0^2 \frac{\partial^2 u}{\partial x^2} \left(1 + \beta \frac{\partial u}{\partial x} + \delta \left(\frac{\partial u}{\partial x} \right)^2 + ... \right) + H\left[\varepsilon, \text{sign}\left(\frac{\partial \varepsilon}{\partial t} \right) \right] \qquad (14)$$

H is a function describing hysteretic nonlinearity, and $\frac{\partial \varepsilon}{\partial t}$ is the strain rate. Note that this function depends on the strain rate and on the strain history as well. However, we should point out that an analytic expression of the H function is still missing the reason for which only few discrete models have been proposed to reproduce and give some understanding of the experimental observations related to nonlinear mesoscopic elastic materials [17–19].

As it was discussed for the classical nonlinearity, the dynamic nonlinear response of NMEM may manifest itself in a variety of ways. Many indicators can therefore be defined to link the detected strain amplitude of the driving frequency to resonance shift, harmonics amplitude, break of the superposition principle, etc. In that case, additional indicators not existing for classical nonlinear materials can be introduced, in the sense that the observed effects on mesoscopic materials might be very different depending on the excitation duration (seconds, minutes, etc.). Therefore, two categories of experiments can be defined: fast dynamics, when the experiment lasts one or few periods of the perturbation, and slow dynamics when the response of the system is tracked on much longer time scale to observe conditioning and relaxation.

3.1 Fast dynamics

During a dynamic experiment, fast dynamic effects appear rapidly (the very early pico or nanoseconds are sufficient to observe the amplitude dependence) and could be observed using standing or transient waves.

Harmonic generation consists in exciting a sample with a source function and analyzing signals detected by receivers in the frequency domain by determining harmonic amplitudes via a Fourier analysis. Most experiments were conducted using compressional waves; however, some bending [20] and torsional wave measurements have been conducted as well [21].

The plot of the second and third harmonic amplitudes as a function of the strain amplitude of the fundamental remains a power law $y = ax^b$, as for classical nonlinearity. However, the calculation of the slope b of the same curve plotted in logarithmic scale provides a new quantitative information (i.e., in contradiction with what theoretically expected), certainly linked to the nature of the nonlinearity, where the exponent revealed to be the same for the second and third harmonics. In addition, for the same dynamic strain, the amplitude of the third harmonic (i.e., odd harmonics) is larger than the one corresponding to the second harmonic (i.e., even harmonics).

3.2 Nonlinear resonance frequency shift

Nonlinear effects can also be determined through the amplitude dependence of the resonance frequency through the technique named nonlinear resonant ultrasound spectroscopy (NRUS). The amplification provided by resonance makes

NRUS one of the most sensitive ways to observe nonlinear behavior, even at small dynamic strains ($\varepsilon \sim 10^{-8}$). In general, we can excite resonances by sweeping upward and downward around a given resonance frequency, and frequency sweeps are repeated at successively increasing amplitude over the same frequency interval. The frequency shift resulting from the different strain amplitudes helps learning about the nature of nonlinearity. Note that the dependence of the normalized frequency shift on the strain is a power law $y = ax^b$, where the exponent measured in different experiments revealed to be ($b = 1$) again different from the prediction of the classical Landau theory.

3.2.1 Slow dynamic effects

Slow dynamics is by far the most typical characteristic of the nonclassical NMEM. It refers to the logarithm dependence recovery of the elastic modulus to the original initial value (i.e., at rest) after being excited and therefore softened by a large amplitude strain. The log-time evolution of the elastic modulus resembles to a creep-like behavior observed in quasi-static experiments. However, it is important to note that slow dynamics is more likely a *new creep* behavior due to the fact that modulus is not following the symmetry of the strain. Furthermore, contrary to creep experiments, slow dynamics is a reversible and repeatable behavior, and observations on rocks and some damaged metals are performed at dynamic strain levels two or three orders of magnitude below those of a typical creep experiment. Slow dynamics includes two different scale mechanisms: conditioning and relaxation.

3.2.1.1 Conditioning

Conditioning or softening of the material takes place at dynamic strains corresponding to $\sim 10^{-6}$. Note that full conditioning could be obtained quite rapidly (few seconds to minutes), which seems to be long enough to allow neglecting its effects in fast dynamic experiments (much shorter time-scale). However, experiments show that most of conditioning occurs mostly instantaneously, which makes the coupling between fast dynamics and conditioning unavoidable, in the sense that the same wave propagating in a dynamic experiment is causing non-negligible self-conditioning. The elastic modulus decreases continuously during the dynamic excitation of NMEM until the material reaches a new equilibrium state where no more change takes place (see **Figure 1**). The amount of conditioning depends on the excitation time and amplitude [11, 22].
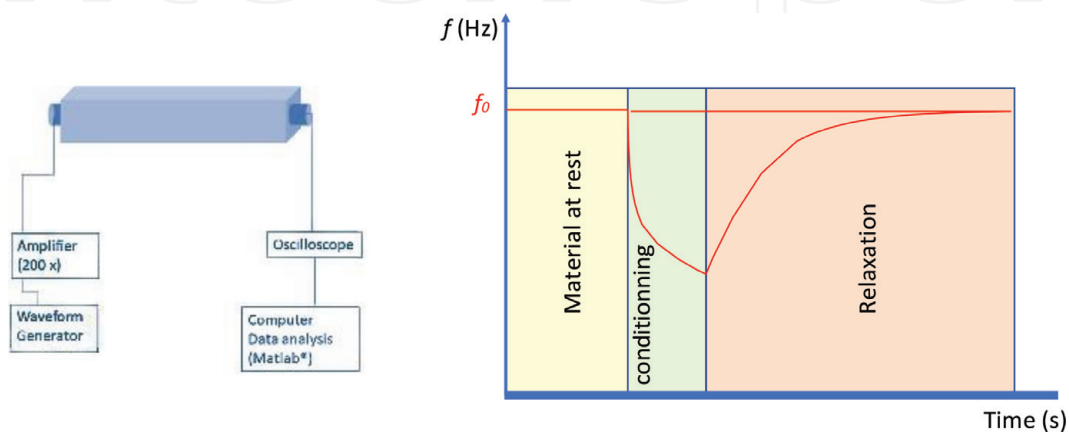

Figure 1.
Scheme of the experimental set-up (left); frequency (or elastic modulus) conditioning and relaxation evolution as a function of time (right).

3.2.1.2 Relaxation

Relaxation starts right after the full conditioning (see **Figure 1**). In practice, a first frequency sweep around a given resonance mode is performed at a small strain amplitude to verify that the material is relaxed (resonance frequency and damping remain unchanged in time). Then, the same excitation is applied at a very large strain level (equivalent to 10^{-6} or 10^{-5}) for few minutes. Afterward, successive sweeps are repeated at the lowest excitation amplitude (linear excitation ~10^{-8}) in order to probe relaxation around the excited resonance mode. Relaxation takes relatively large time and changes as the logarithm of time before the final recovery over minutes, hours, or days depending on the conditioning characteristics (strain amplitude, materials state, strain duration, etc.) [11, 22].

4. Experimental analysis

4.1 Experimental set up

Experiments are conducted generating ultrasonic signals through a waveform generator. Ultrasonic signals defined as monochromatic waves of amplitude A^{inp} and frequency w_0 are used to excite the sample under test not far from one of its compressional resonance mode (the fundamental in general)

$$u(t) = A_{inp} \; cos\,(w_0 t) \tag{15}$$

The emitter transducer is glued to the sample using a linear coupling (phenyl salicylate, for instance). A second (identical) transducer is used to detect the response of the material under test, and it is connected to a digital oscilloscope for data acquisition. Signals are recorded in a short time window once stationary conditions are reached. In order to excite longitudinal modes, the transducers are put, in general, on opposite faces of the samples.

The experimental procedure starts by detecting the output signal at a very low excitation level A^{inp}. The latter is chosen the lowest possible in order to not have any change in the mechanical properties of the material under test. To verify this, we should have a good signal-to-noise ratio to generate output signals emerging from the noise level. In most of the presented experiments, the lowest amplitude was chosen as $A_0^{inp} = 5mV$. Under these conditions, the sample under test behaves almost linearly, and the recorded low amplitude response will be termed as "linear signal" $v_0(t)$. The linear signal measurement, performed without amplification in general, is followed by N acquisitions repeated increasing the amplitude of excitation up to a maximum level. The recorded N signals $v_i(t)$, $(i = 1, .., N)$ are recorded, each corresponding to an excitation amplitude A_i^{inp}.

4.2 The scaling subtraction method (SSM)

Under a dynamic excitation, the presence of nonlinearity can be detected through the validity of the superposition principle, which represents a requirement for a system to be linear. By considering a linear function F, if $v(t) = A\, v_0(t)$ is the input function, we have

$$u_A = F(Av_0) = AF(v_0) = Au_0 \tag{16}$$

F is the transfer function, u denotes the output signal, and A is the amplification factor. Here, u_0 is the response at the excitation amplitude v_0.

Consider an elastic wave propagating in a microdamaged medium. In such a case, one might expect that if the propagation excites the nonlinearity of the system, it will consequently break the superposition property. Therefore, if the exciting wave is generated at amplitude A_0, small enough so that nonlinearity of the medium is negligible, the system will behave linearly and its response is $u_0(t)$. At a larger excitation amplitude A, the response $u(t)$ of the same system is no longer equal to

$$u_{ref}(t) = \frac{A}{A_0} u_0(t) \tag{17}$$

which would be the response of that system if it remains linear even at large amplitudes. Therefore, the difference between the two responses can be taken as an indicator of nonlinearity. The nonlinear scaled subtracted signal $w(t)$, termed SSM signal, is introduced as (see **Figure 2**)

$$w(t) = u(t) - u_{ref}(t) \tag{18}$$

This time domain analysis of elastic nonlinearity, called scaling subtraction method (SSM), has proved to be sensitive to damage detection and easy to set [16].

From the quantitative point of view, if exciting signals are in the form of monochromatic continuous waves and measurements are taken in standing wave conditions, the SSM signal $w(t)$ is also a continuous wave. Thus, a parameter could be introduced either as the maximum or the "energy" of the nonlinear signal $w(t)$ as

$$\theta = \max(w(t)) \tag{19}$$

$$\theta' = 1/T \int_0^T w^2(t)dt \tag{20}$$

where T is the wave period. The parameter could then be shown as a function of excitation amplitude in order to highlight nonlinearity.

From the point of view of damage monitoring, for a given sample state, a quantitative nonlinear indicator must be defined. To this purpose, we observe that in materials exhibiting hysteresis, a power law holds in the form

$$\theta = ax^b \tag{21}$$

where x is the maximum of the output amplitude. Thus, experimental data could be fitted to derive the coefficient a and the parameter b, normally called slope, since
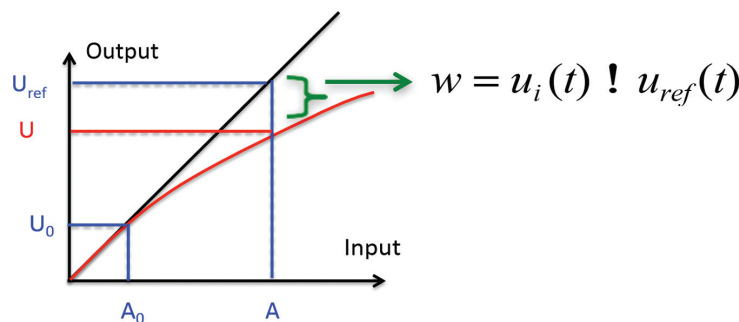

Figure 2.
Basic principle of SSM analysis.

in log-log scale, the above equation reduces to a straight line $20\ log_{10}\ \theta = a'$ $+\ b20\ log_{10}\ x$.

As an alternative, the nonlinear indicator could be defined as the value of θ at a fixed value of x (excitation level).

5. Application to nonlinear characterization of concrete

Consolidated granular media and in particular concrete exhibit a strong nonlinear hysteretic elastic behavior when excited by ultrasonic wave perturbations [23–28]. The nonlinear behavior is strongly enhanced when the concrete is damaged [29]. A significant enhancement of the nonlinear response can be created by one of the numerous damages that might occur within concrete structures via quasi-static loading [30, 31], thermal stresses [8, 32, 33], carbonation [34], corrosion [35], and salt expansion [36]. Here, we show how different damage types affect the nonlinear observations derived from the scaling subtraction method, thus suggesting SSM to be a suitable method to monitor damage evolution in time. We also wish to highlight how nonlinear indicators defined using the SSM approach (particularly the slope b) allow to discriminate between different types of damage.

5.1 Load effects on discontinuities in concrete

One of the major effects that create damage in concrete is the application of mechanical loads in the presence of discontinuities. Indeed, discontinuity surfaces are very often the place from where damage may begin its progression. The effects could be the increase in crack density [37] and/or the crack openings [38, 39], depending on the nature of discontinuity such as existing cracks [40] or weak layers [41–43].

In [25], one specimen with an internal discontinuity surface was produced by piling up two concrete cubes (measuring 10 cm on each side). The two pieces were joined using a thin layer of cement paste. Concrete cubes were produced using a concrete mix with CEM II A-L 42.5 R cement, ordinary aggregates (max. size = 16 mm) and a water to cement ratio equal to 0.74, with no admixtures. Their age at the date of testing was approximately 6 months. The evaluation of the mechanical characteristics of the concrete was performed using mono-axial static compression tests that resulted in a compressive strength of 24 N/mm^2. The longitudinal wave speed in the cube was measured to be $V = 3850 m/s$ and the density of the cubes $\rho = 2330\ kg/m^3$. For this experiment, one emitter (T1) and three receivers (R2, R3, and R4) were used, as schematized in **Figure 3**. Two receivers (R2 and R3) performed direct transmission measurements; whereas, the third (R4) was used in indirect transmission mode. It is important to note that the direct path from the emitter to R2 and R4 crosses the discontinuity of the concrete, while the path to receiver R3 does not (See **Figure 3**). Only the results obtained from receiver R4 will be shown here for the sake of conciseness.

As explained above, the evolution of damage as a function of the applied load can be followed using different nonlinear indicators. However, in these experiments, it is important to note that the frequency analysis (using FFT for instance) was not efficient, since the nonlinear indicators related to the possible generated frequencies (higher order harmonics) were below the noise level. Therefore, the application of the traditional nonlinear elastic wave spectroscopy is not expected to be efficient in detecting the presence of nonlinearity during these experiments.
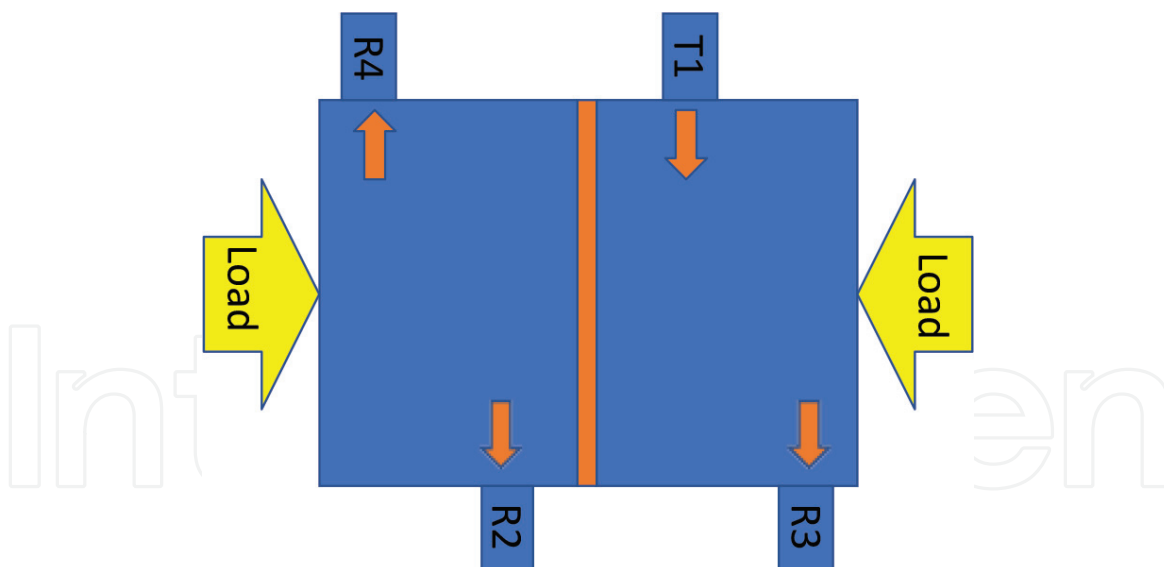
Figure 3.
Experimental set-up based on the use of four identical transducers, one transmitter (T1), and three receivers (R2, R₃, and R₄).

In general, when comparing different signals at different load levels, even if we observe a change in the signal shape, we should keep in mind that the change might not be due only to the damage of the interface, but also due to the other effects such as a change in the coupling quality or in the transducers arrangement especially when detaching and reattaching transducers. In that sense, it is important to note that the nonlinearity indication provided by the SSM represents an absolute measure since the reference signal is contained in the measurement itself.

Experimental results from [25] are shown in **Figure 4**. As anticipated above, the latter refers to signals recorded by the receiver R_4. The SSM indicator (θ) shows that the increase of load does not immediately cause a raise of nonlinearity, which starts to increase slightly only from 10 to 50 kN. However, we notice a clear increase in θ for higher loads, when the specimen is close to collapse, where fractures close to the bonding layer become evident around 90 kN. The log-log scale of θ on the same figure shows that θ changes linearly as a function of the amplitude. The slope of this logarithm evolution, which is around ~2 at low loading steps, becomes ~3 for higher load levels. Therefore, the evolution of nonlinearity as a function of damage progression can be appreciated, for a fixed value of the input energy, by analyzing the nonlinear indicator as a function of the applied load. This is done by extrapolating θ from the fitting function in order to obtain ($\theta(x_0)$) at each loading step.

The trend presented in **Figure 4** leads to the following conclusions. The low compressive loads create a rearrangement of the internal structure (e.g., pores closing) where the damage in the discontinuity is expected to be minor. When loads are increased (up to ~50% of the failure load), the nonlinearity increases slightly, and early damage (microdamage) is expected in the discontinuity. Finally, macrodamage is created at loads larger than ~50% of the failure load, where a clear change of the slope is observed.

5.2 Corrosion effect on elastic properties of reinforced concrete

Steel corrosion in reinforced concrete elements has negative effects on their load carrying capacity [44]. Furthermore, the expansion of the oxidation products creates cracking [45, 46] and deteriorates the bond between steel and concrete [47]. The overall weakening of the concrete structures by reinforcement corrosion is then expected [48].
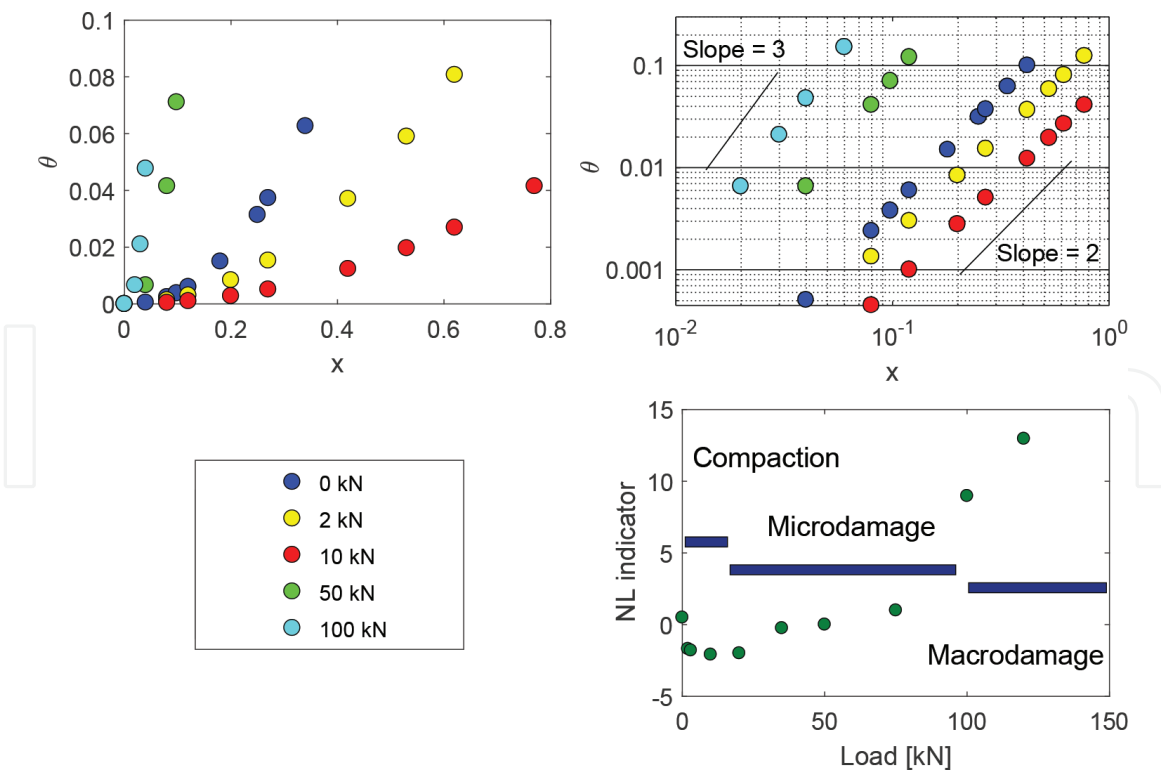
Figure 4.
Evolution of the SSM indicator θ as a function of energy of the output signal in the case of the low-quality layer discontinuity.

In [35], ultrasonic tests were performed on one reinforced concrete sample sizing ($90 \times 90 \times 500$ mm^3), which contained a steel bar (14 mm of diameter) located approximately in its center, making a reinforcement ratio corresponding to 0.19% (see **Figure 5**). Ultrasonic measurements consisted in exciting the sample using sinusoidal bursts at increasing amplitudes (10 cycles of 55.5 kHz frequency). Ultrasonic measurements were performed at different corrosion steps, as induced by an accelerated corrosion set-up, and data analysis was made on the basis of linear and nonlinear indicators. Linear indicators were the ultrasonic phase velocity (compression mode) and attenuation. Linear wave velocity was determined using the lowest excitation amplitude. Since transducers were removed before the beginning of each accelerated corrosion step, it was preliminarily verified that effects due to small differences in coupling were negligible compared to the ones induced by corrosion. Transducer positioning was made in such a way to be able to detect the direct transmission of the traveling ultrasonic wave. Furthermore, another transducer was put on the same side as the transmitter (at ~15 cm) in order to estimate the sensitivity of the proposed techniques when the access to the opposite face is not possible.
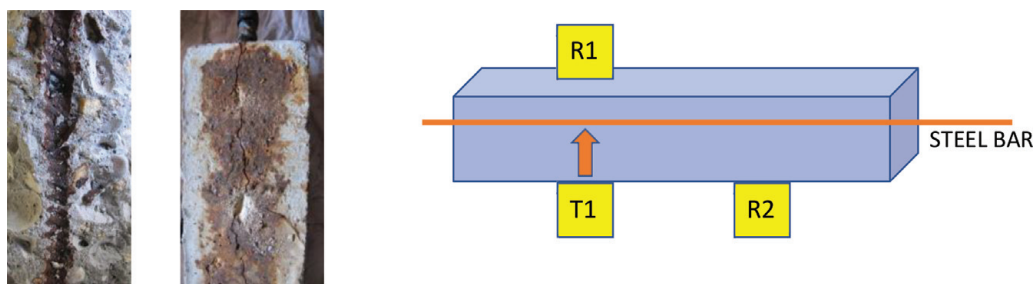

Figure 5.
Reinforced concrete samples affected by an important corrosion (left); ultrasonic transmitters and receivers placed on the concrete sample (right).

At the time when linear indicators, namely ultrasonic velocity and attenuation, manifested a weak sensitivity to corrosion (the velocity regularly but slightly decreases and the attenuation increases), the nonlinear indicator showed an important evolution. Indeed, the relative variations corresponding to velocity and attenuation as a function of the corrosion step were determined as 4 and 70% at most, respectively. However, larger effects were observed for the relative variation of the nonlinear indicator by changing up to 350%. Here, it should be pointed out that when comparing the first and the last corrosion steps (instead of considering as reference the intact sample), the relative change of the velocity and attenuation were 1.5 and 30%, respectively, while the nonlinear indicator was ∼250%. This evolution shows the high sensitivity of nonlinear methods to the microstructure modifications due to corrosion. Finally, the nonlinear indicator remains sensitive to corrosion creation and evolution even when the access to the opposite side of the corroded concrete samples is not possible. Indeed, **Figure 6** shows that the nonlinear indicator extracted from data of receivers 1 and 2 was almost the same at the first two stages of corrosion. For the last two corrosion states, a difference can be noticed between both results, but the increase of sensitivity to corrosion is clearly visible for both sensors.

5.3 Thermally induced damage in concrete

Thermal stresses are a further cause of damage formation in concrete. To analyze the efficiency of the SSM in monitoring evolution of damage due to heating, mortar samples of size $25 \times 25 \times 100$ mm^3 were prepared in [8]. Ordinary Portland cement (CEM I 42.5N) was used with aggregates from alluvial sand, with well-rounded particles and dry density of 2659 kg m^3. The amount of aggregates in the mortar was about 40% by volume, corresponding to a cement-to-aggregate ratio (c/a) by a mass fraction of 0.917. Water-to-cement ratio (w/c) was chosen as 0.3 by mass. Samples with larger and smaller grains were prepared.

Samples were heated in an oven at different temperature levels and ultrasonically monitored at each temperature level after having removed from oven and let cool down to room temperature. A linear analysis was applied measuring time of
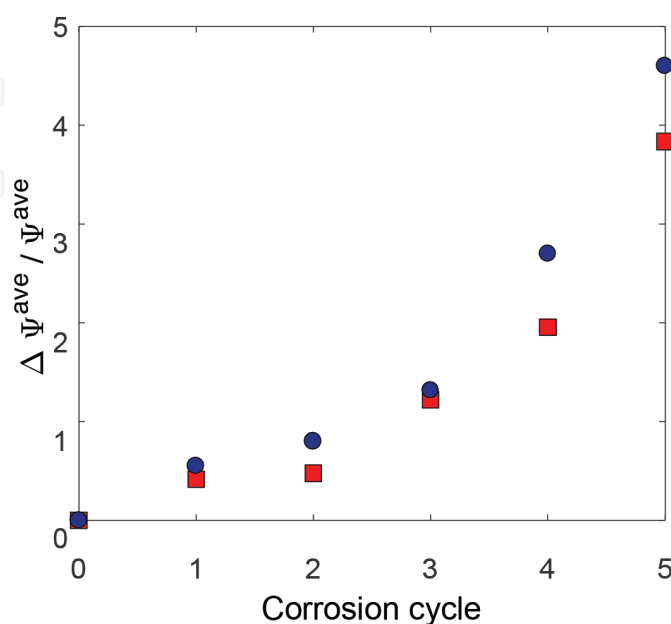

Figure 6.
Relative variations of the nonlinear indicator (with respect to the uncorroded initial state) as a function of the corrosion step. Squares and circles correspond to data recorded by receivers 1 and 2, respectively.

flight, but it proved to be only slightly sensitive to the increase of damage and without any difference in the behavior of samples with small and large aggregates sizes.

Thus, in order to appreciate the different behaviors expected for the different samples, the SSM technique was applied as discussed previously, with ultrasonic sensors attached on the bases of the sample prisms. Results are reported in **Figure** 7, where the nonlinear parameter is shown vs. the output amplitude. It is possible to observe that damage starts earlier in the sample with large aggregates, as expected. Macrocracks are more rapidly formed and at the largest thermal excitation, the increase in nonlinearity is noticeable.

Furthermore, it is also possible to observe a change in slope (nonlinear indicator b) when macrocracks start appearing (large aggregates case only). This is similar to what observed for the case of quasi-static loadings. Indeed, in both quasi-static and thermal cases, the situation is similar: microcracking (first) and coalescence into macrocracks (later) is due to the presence of localized mechanical stresses (due to load or local gradients of thermal expansion), without the formation of any reaction products, as in the cases of corrosion and salt expansion (see next subsection).

5.4 Degradation by expansive salts in masonry systems

The presence of soluble salts into capillary water is one of the major problems affecting masonry structures. Numerous works pointed out the potential noxiousness of water-transported salts (which might happen during repeated wet-dry cycles). Indeed, due to crystallization of some salts in the form of expansive compounds, progressive cracking and detachment phenomena happen especially at the interfaces between different material layers. In that sense, there is a clear need to develop an effective and reliable diagnosis of the onset of such damage phenomena in order to make corrective actions, in terms of repair and maintenance optimization, possible [49–53]. The close interaction between the ultrasonic wave and the material mechanical/elastic properties made ultrasonic methods widely used for
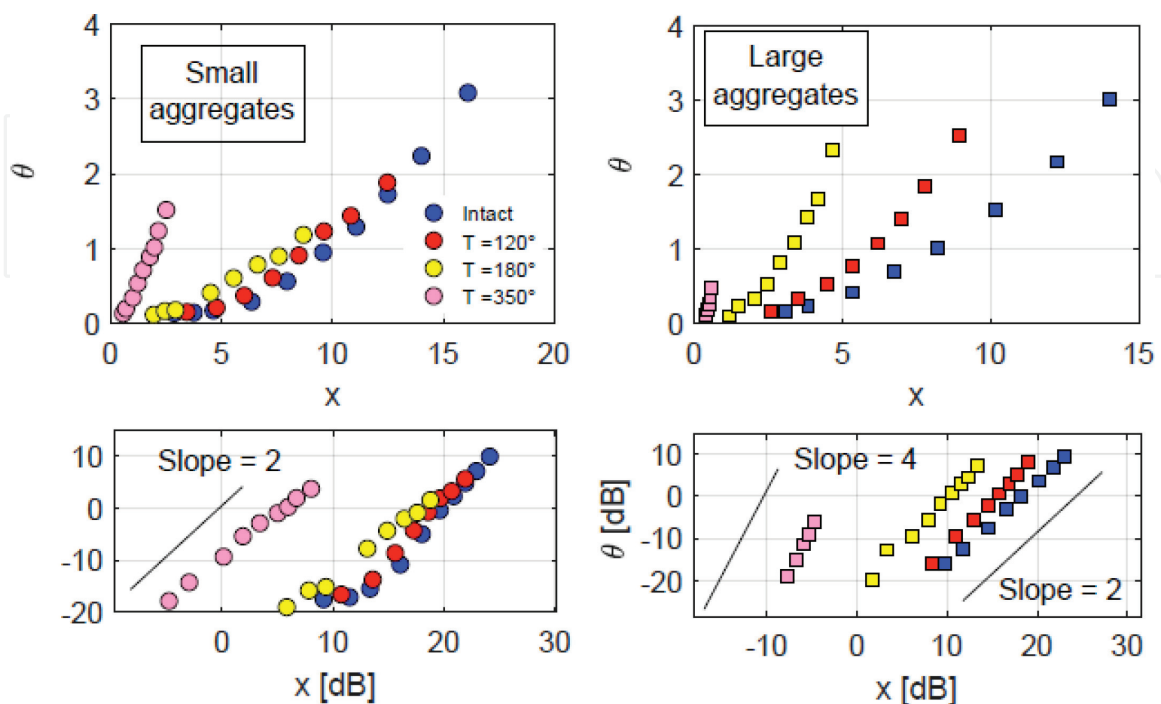

Figure 7.
Nonlinear parameter vs. output amplitude for samples with small and large aggregates at different levels of thermal damage.

damage characterization in civil engineering, in particular when dealing with cement-based materials. However, it has been remarked that ultrasonic pulse velocity, dispersion, and attenuation phenomena in concrete and multiphase materials in general are only considered in the linear regime at the time when without taking into account any possible dependence on the excitation amplitude [54–56]. Indeed, degradation of material mechanical properties can be more easily detected using nonlinear ultrasounds, which is significantly more sensitive at the very early damage stages than traditional linear ultrasonic techniques.

In [36], the sensitivity of the SSM was investigated, with respect to its application to the characterization of damage induced by the crystallization of expansive salts in masonry systems. Salt crystallization in coupled brick-mortar specimens was carried out through a damage protocol, which consisted of repeating cycles of imbibition in a salt solution followed by a drying phase. Specimens were manufactured by coupling a clay brick with two external layers of dehumidifying mortar using commercially available bricks in order to be representative of most common building products. A hand-molding procedure was used with natural drying and subsequent baking at the temperature of 1030°C. Irregular prismatic shape sizing $240 \times 115 \times 63$ mm^3, lightly sanded on the outside surface, was then obtained. In analogy with typical restoration systems, a dehumidifying mortar was used for the external layers of the specimens in order to protect the underlying masonry from capillary rising dump, in the presence of soluble salts.

Recommendations from Standard UNI EN 12370 were used as a starting point for producing an accelerated decay protocol on the lab specimens. Then, the following damage protocol is applied.

- Immersion in a solution (14% of Na_2SO_4, by weight), for 2 h at $(20 \pm 0.5^\circ C)$.

- Heating at $85 \pm 5^\circ C$ during $\sim$14 h.

- Heating at $105 \pm 5^\circ C$ during $\sim$4 h.

- Cooling at room temperature during $\sim$2 h.

Direct transmission of longitudinal ultrasonic waves was performed using two identical piezoelectric transducers with a central frequency of 55.5 kHz and 40 mm diameter (see scheme in **Figure 8**). Input bursts are composed of 10 sine cycles with a frequency of 55.5 kHz and fixed amplitude. Then, the excitation amplitude was progressively increased for successive bursts: for each damage step, the excitation amplitudes ranged between 1 and 20 V, before amplification. A time window of 200 ms was used for the acquisition of the received waveforms, and only first arrivals were considered in the analysis.

Figure 9 shows the evolution of the nonlinear effects caused by damage accumulation. Indeed, through the latter, it is possible to see the change in the rise of the nonlinear parameter as a function of the excitation energy when damage increases. Indeed, the power law evolution shows that the necessary amount of the excitation energy to trigger the nonlinear behavior decreases as a function of damage. Note that during the same damage steps, almost no mass variation occurred. This means that the brick-mortar adherence of the tested specimen ensured a very good resistance to damage growth during the first imbibition-drying cycles. On the other hand, the SSM analysis is in accordance with the mass variation measurements. Indeed, the semi-log plot of the same curve shows that the slope remains unchanged (approximately 2) during the first damage steps (partially cracked specimen), and the presence of first cracks (or microcracks) increases the sensitivity of the SSM

Figure 8.
Experimental set-up for ultrasonic characterization tests.
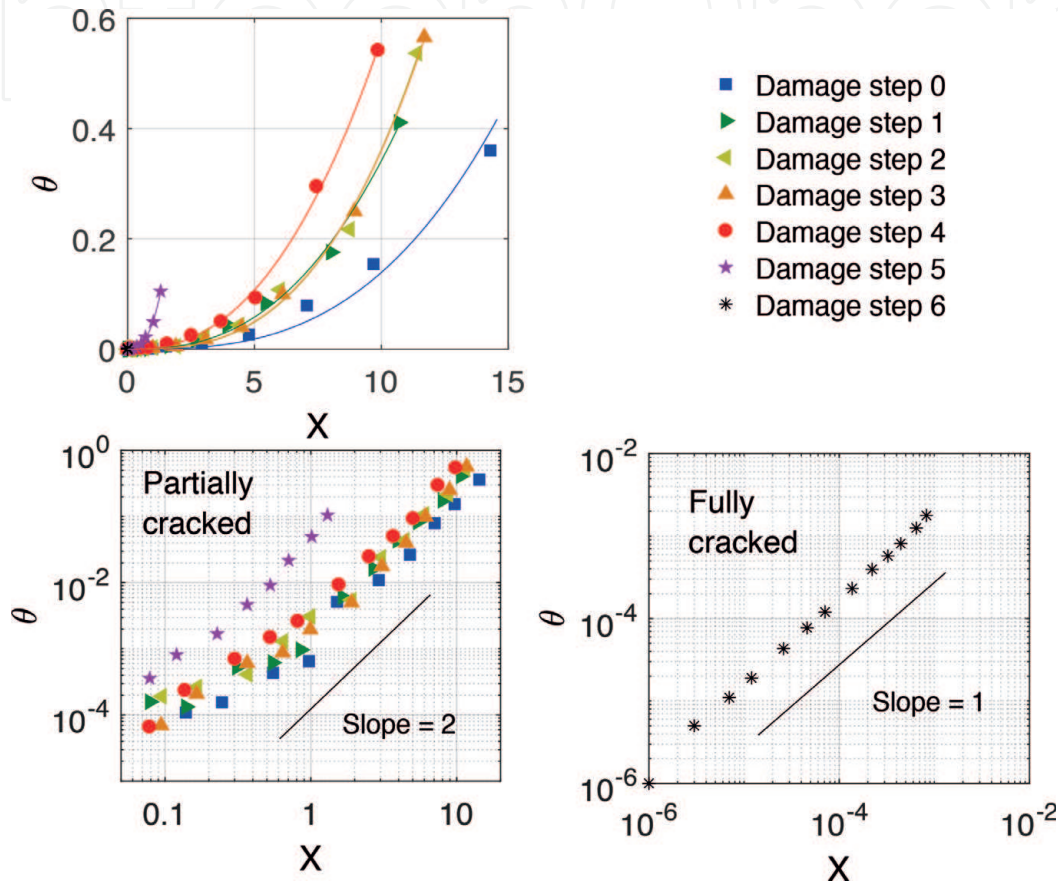

Figure 9.
Evolution of the nonlinear parameter vs. normalized energy at increasing degradation steps by expansive salts.

parameter without changing the power law behavior. At the end of the damage steps (fully cracked sample), a clear change of the slope can be noticed, since it goes from ∼2 to ∼1, again in accordance with the mass variation measurements.

6. Conclusion

In this chapter, we analyzed effects of different types of damage on the nonlinear properties of concrete using longitudinal direct transmission mode measurements. Our results suggest that, despite the damage origin (mechanical stress, thermal actions, corrosion, etc.), nonlinear ultrasonic measurements could be a useful tool for monitoring damage. In particular, the analysis performed in the time domain using the scaling subtraction method allows obtaining a sufficiently large signal-to-noise ratio, which is not always the case with standard analysis in the frequency domain. Furthermore, the high sensitivity to the appearance of degradation allows to provide precursory indications with approaching rupture. Further

studies will be performed to exploit the possibility of using our approach to assess full-scale structures where, beyond the technical problems, we still need to perform a real strategy to choose the proper excitation frequency in order to overcome difficulties related to material attenuation.

Author details

Mourad Bentahar[1*], Charfeddine Mechri[1,2], Paola Antonaci[3], Antonio Gliozzi[4] and Marco Scalerandi[4]

1 LAUM, CNRS, Université du Maine, Le Mans, France

2 CTTM, Le Mans, France

3 Department of Structural, Geotechnical and Building Engineering, Politecnico di Torino, Torino, Italy

4 Department of Applied Science and Technology, Politecnico di Torino, Torino, Italy

*Address all correspondence to: mourad.bentahar@univ-lemans.fr

References

[1] Cantrell J, Yost W. Acoustic harmonic generation from fatigue induces dislocation dipoles. Philosophical Magazine. 1996;**69**: 315-326

[2] Moussatov A, Castagnéde B, Gusev V. Frequency up-conversion and frequency down-conversion of acoustic waves in damaged materials. Physics Letters A. 2002;**301**:281-290

[3] Zaitsev V, Nazarov V, Tournat V, Gusev V, Castagniéde B. Luxembourg-Gorky effect in a granular medium: Probing perturbations of the material state via cross-modulation of elastic waves. Europhysics Letters. 2005;**70**: 607-613

[4] Bentahar M, El Guerjouma R. Monitoring progressive damage in polymer-based composite using nonlinear dynamics and acoustic emission. The Journal of the Acoustical Society of America. 2009;**125**:39-44

[5] Muller M, Sutin A, Guyer R, Talmant M, Laugier P, Johnson P. Nonlinear resonant ultrasound spectroscopy (NRUS) applied to damage assessment in bone. The Journal of the Acoustical Society of America. 2005;**118**:3946-3952

[6] Van Den Abeele KE-A, Carmeliet J, Tencate J, Johnson P. Nonlinear elastic wave spectroscopy (NEWS) techniques to discern material damage. Part II: Single mode nonlinear resonance acoustic spectroscopy. Research in Nondestructive Evaluation. 2000;**12**:31-42

[7] Mechri C, Scalerandi M, Bentahar M. Enhancement of harmonics generation in hysteretic elastic media induced by conditioning. Communications in Nonlinear Science and Numerical Simulation. 2017;**45**:117-128

[8] Scalerandi M, Griffa M, Antonaci P, Wyrzykowski M, Lura P. Nonlinear elastic response of thermally damaged consolidated granular media. Journal of Applied Physics. 2013;**113**:154902

[9] Zinszner B, Johnson PA, Rasolofosaon PNJ. Influence of change in physical state on elastic nonlinear response in rock: Significance of effective pressure and water saturation. Journal of Geophysical Research. 1997; **102**:8105-8120

[10] Baccouche Y, Bentahar M, Mechri C, Novak A, El Guerjouma R. Nonlinear analysis of damaged metal-based composite plates using guided waves. Acta Acustica United with Acustica: Aims and Scope. 2017;**103**:967-977

[11] Bentahar M, El. Aqra H, El Guerjouma R, Griffa M, Scalerandi M. Hysteretic elasticity in damaged concrete: quantitative analysis of slow and fast dynamics. Physical Review B. 2006;**73**:014116

[12] Tencate J et al. Nonlinear and nonequilibrium dynamics in geomaterials. Physical Review Letters. 2004;**93**:065501

[13] Johnson PA, Sutin A. Slow dynamics and anomalous nonlinear fast dynamics in diverse solids. The Journal of the Acoustical Society of America. 2005;**117**: 124-130

[14] Aleshin V, Van Den Abeele K. Microcontact-based theory for acoustics in microdam-aged materials. Journal of the Mechanics and Physics of Solids. 2007;**55**:765-787

[15] Darling TW, Tencate JA, Sven V, et al. Localizing nonclassical nonlinearity in geological materials with neutron scattering experiments. In: Innovations in Nonlinear Acoustics: AIP Conference Proceedings. Vol. 838; 2006. pp. 12-19

[16] Johnson PA, Rasolofosaon PNJ. Manifestation of nonlinear elasticity in rock: Convincing evidence over large frequency and strain intervals from laboratory studies. Nonlinear Processes in Geophysics. 1996;**3**:77-88

[17] Scalerandi M, Delsanto PP. Modeling nonclassical nonlinearity, conditioning, and slow dynamics effects in mesoscopic elastic materials. Physical Review B. 2003;**68**:064107

[18] Shkerdin G, Glorieux C. Nonlinear modulation of lamb modes by clapping delamination. The Journal of the Acoustical Society of America. 2008;**124**:3397-3409

[19] Gusev V, Castagnède B, Moussatov M. Hysteresis in response of nonlinear bistable interface to continuously varying acoustic loading. Ultrasonics. 2003;**41**:643-654

[20] Baccouche Y, Bentahar M, Mechri C, El Guerjouma R. Hysteretic nonlinearity analysis in damaged composite plates using guided waves. Journal of Acoustical Society of America. 2013;**133**(4):EL256-EL261

[21] Bonner BP, Berge P, AracneâRuddle C, Boro C, Hardy E, Trombino C. Ultrasonic characterization of synthetic soils for application to near surface geophysics. In: Proceedings of the Symposium on the Application of Geophysics to Engineering and Environmental Problems; 1999. pp. 455-463

[22] Scalerandi M, Gliozzi AS, Bruno CLE, Antonaci P. Nonequilibrium and hysteresis in solids: Disentangling conditioning from nonlinear elasticity. Physical Review B. 2010;**81**:104114

[23] Bruno CLE et al. Analysis of elastic nonlinearity using the scaling subtraction method. Physical Review B. 2009;**79**:064108

[24] Shah AA, Ribakov Y. Non-destructive evaluation of concrete in damaged and undamaged states. Materials and Design. 2009;**30**: 3504-3511

[25] Antonaci P, Bruno CLE, Bocca PG, Scalerandi M, Gliozzi AS. Nonlinear ultrasonic evaluation of load effects on discontinuities in concrete. Cement and Concrete Research. 2010;**40**:340-346

[26] Hilloulin B et al. Small crack detection in cementitious materials using nonlinear coda wave modulation. NDT and E International. 2014;**68**: 98-104

[27] Quang AV et al. Concrete cover characterization using dynamic acousto-elastic testing and Rayleigh waves. Construction and Building Materials. 2016;**114**:87-97

[28] Aggelis D, Momoki S, Shiotani T. Experimental study of nonlinear wave parameters in mortar. Construction and Building Materials. 2013;**47**:1409-1413

[29] Garnier V et al. Acoustic techniques for concrete evaluation: Improvements, comparisons and consistency. Construction and Building Materials. 2013;**43**:598-613

[30] van den Abeele K, De Visscher J. Damage assessment in reinforced concrete using spectral and temporal nonlinear vibration techniques. Cement and Concrete Research. 2000;**30**: 1453-1464

[31] Antonaci P, Bruno CLE, Gliozzi AS, Scalerandi M. Monitoring evolution of compressive damage in concrete with linear and nonlinear ultrasonic methods. Cement and Concrete Research. 2010; **40**:1106-1113

[32] Payan C et al. Quantitative linear and nonlinear resonance inspection techniques and analysis for material characterization: Application to

concrete thermal damage. The Journal of the Acoustical Society of America. 2014;**136**:537-546

[33] Park S-J, Yim HJ, Kwak H-G. Effects of post-fire curing conditions on the restoration of material properties of fire-damaged concrete. Construction and Building Materials. 2015;**99**:90-98

[34] Bouchaala F, Payan C, Garnier V, Balayssac JP. Carbonation assessment in concrete by nonlinear ultrasound. Cement and Concrete Research. 2011;**41**:557-559

[35] Antonaci P, Bruno CLE, Scalerandi M, Tondolo F. Effects of corrosion on linear and nonlinear elastic properties of reinforced concrete. Cement and Concrete Research. 2013;**51**:96-103

[36] Antonaci P, Formia A, Gliozzi AS, Scalerandi M, Tulliani JM. Diagnostic application of nonlinear ultrasonics to characterise degradation by expansive salts in masonry systems. NDT and E International. 2013;**55**:57-63

[37] Paliwal B, Ramesh KT. An interacting micro-crack damage model for failure of brittle materials under compression. Journal of the Mechanics and Physics of Solids. 2008;**56**:896-923

[38] Galvez JC, Cervenka J, Cendonc DA, Saouma V. A discrete crack approach to normal/shear cracking of concrete. Cement and Concrete Research. 2002;**32**:1567-1585

[39] Zhang J, Li VC. Simulation of crack propagation in fiber-reinforced concrete by fracture mechanics. Cement and Concrete Research. 2004;**34**:333-339

[40] Barpi F, Valente S. Modeling water penetration at dam-foundation joint. Engineering Fracture Mechanics. 2008;**75**:629-642

[41] Djazmati B, Pincheira JA. Shear stiffness and strength of horizontal construction joints. ACI Structural Journal. 2004;**101**:484-493

[42] Sharif A, Rahman MK, Al-Gahtani AS, Hameeduddin M. Behaviour of patch repair of axially loaded reinforced concrete beams. Cement and Concrete Composites. 2006;**28**:734-741

[43] Mangat PS, O'Flaherty FJ. Influence of elastic modulus on stress redistribution and cracking in repair patches. Cement and Concrete Research. 2000;**30**:125-136

[44] Cairns J, Zhao Z. Behavior of concrete beams with exposed reinforcement. Journal of Structural Engineering. 1999;**99**:141-154

[45] Seok JB, Hwan OB. Effects of non-uniform corrosion on the cracking and service life of reinforced concrete structures. Cement and Concrete Research. 2010;**40**:1441-1450

[46] Care S et al. Times to cracking in reinforced mortar beams subjected to accelerated corrosion tests. Materials and Structures. 2010;**43**:107-124

[47] Fang C et al. Corrosion influence on bond in reinforced concrete. Cement and Concrete Research. 2004;**34**:2159-2167

[48] Masayasu O, Uddin FAKM. Mechanisms of corrosion-induced cracks in concrete at meso- and macro-scales. Journal of Advanced Concrete Technology. 2008;**6**:419-429

[49] Rirsch E, Zhang Z. Rising damp in masonry walls and the importance of mortar properties. Construction and Building Materials. 2010;**24**:1815-1820

[50] Lubelli B, Van Hees RPJ, Groot CJWP. The role of sea salts in the occurrence of different damage mechanisms and decay patterns on brick masonry. Construction and Building Materials. 2004;**18**:119-124

[51] Brocken H, Nijland TJ. White efflorescence on brick masonry and concrete masonry blocks, with special emphasis on sulfate efflorescence on concrete blocks. Construction and Building Materials. 2004;**18**:315-323

[52] Fassina V et al. Evaluation of compatibility and durability of a hydraulic lime-based plaster applied on brick wall masonry of historical buildings affected by rising damp phenomena. Journal of Cultural Heritage. 2002;**3**:45-51

[53] Abu-Zei N et al. Non-invasive characterization of ancient foundations in Venice using the electrical resistivity imaging technique. NDT and E International. 2006;**39**:67-75

[54] Komlos K et al. Ultrasonic pulse velocity test of concrete properties as specified in various standards. Cement and Concrete Composites. 1996;**18**: 357-364

[55] Kim YH, Lee S, Kim HC. Attenuation and dispersion of elastic waves in multi-phase materials. Journal of Physics D. 1991;**24**:1722-1728

[56] Landis E, Shah S. Frequency-dependent stress wave attenuation in cement-based materials. Journal of Engineering Mechanics. 1995;**121**: 737-743